Inorg. Chem. **1989**, *28*, 3519–3523

Contribution from the Department of Chemistry and Biochemistry,
University of California, Los Angeles, California 90024-1569

Calculation of Excited-State Distortions and the Missing-Mode Effect from the High-Resolution Emission Spectrum of *trans*-$W(N_2)_2(dppe)_2$

Londa J. Larson and Jeffrey I. Zink*

Received January 23, 1989

The emission spectra of solid *trans*-$W(N_2)_2(dppe)_2$ taken at 19 K with 514.5-nm excitation exhibits sharp-line vibronic structure with line widths as narrow as 15 cm^{-1}. Thirteen normal vibrational modes contribute to the spectrum. The vibrational spacings in the 19 K solid spectrum are assigned to normal modes, which are independently determined by Raman spectroscopy. The distortions of the molecule in its first excited state are calculated by using Heller's time-dependent theory of molecular spectroscopy. Distortions of 0.01, 0.03, and 0.007 Å are calculated for the W–P, W–N, and N–N bonds, respectively. In a 2-methyltetrahydrofuran (2-MeTHF) glass or for the solid at 79 K, the structure broadens into one regularly spaced progression. This progression is an example of the missing-mode effect (MIME). The MIME is quantitatively analyzed by using the frequencies and displacements determined from analysis of the sharp-line emission spectrum.

The excited-state properties of *trans*-$W(N_2)_2(dppe)_2$ (dppe = 1,2-bis(diphenylphosphino)ethane) have been the focus of several recent spectroscopic[1-3] and photochemical studies.[4-8] This complex exhibits novel photochemistry, undergoing alkylation reactions in the presence of alkyl halides. On the basis of the spectroscopic studies, the lowest energy excited state was assigned to a spin-forbidden transition from a metal to dppe charge-transfer (MLCT) excited state. All of the reported studies of the luminescence were carried out in glassy media (2-MeTHF). At temperatures between 8 and 80 K, the spectra contain one apparent vibronic progression with a spacing of about 500 cm^{-1}.[3]

We have discovered that the emission spectrum of solid *trans*-$W(N_2)_2(dppe)_2$ at 19 K exhibits sharp-line vibronic structure. When the sample temperature is raised to liquid-nitrogen temperature, one apparent progression is observed that cannot be attributed to a single normal vibrational mode of the molecule. The vibronic spacings in the higher temperature solid emission are the same as those observed in the glass spectrum. This progression is an example of the missing-mode effect (MIME).

The MIME is a regularly spaced vibronic progression in an electronic spectrum that does not correspond to any ground-state normal vibrational mode of the molecule.[9-15] The observed progression does not result from a single mode but depends on all of the normal modes that are displaced significantly in the excited state. The MIME in the electronic spectra of $Ph_2PS_2N_3$, $W(CO)_5$(pyridine), and $K_2[PtCl_4]$ has been quantitatively characterized.[10-15] In these compounds the modes contributing to the MIME were determined from Raman spectra.

In this paper we report that the emission spectrum of a solid sample of *trans*-$W(N_2)_2(dppe)_2$ at 19 K exhibits much more highly resolved structure than that which can be observed from a 2-MeTHF glass at temperatures as low as 8 K.[3] Line widths of 15 cm^{-1} are observed. The structure is broadened, giving rise to a MIME frequency of approximately 500 cm^{-1} when the sample is in a 2-MeTHF glass or when the solid is raised to liquid-nitrogen temperature. The molecular distortions that the molecule undergoes in its first excited state are determined from the highly resolved spectrum by using Heller's time-dependent theory of molecular spectroscopy. We then quantitatively analyze the MIME using these distortions.

Experimental Section

trans-$W(N_2)_2(dppe)_2$ was prepared according to the literature method[16] in the laboratory of Professor Horst Kisch at the University of Erlangen, FRG.

Emission Spectra. Samples were mounted in a Displex closed-cycle helium refrigeration unit equipped with a thermocouple and a heater. Time-resolved emission spectra were taken of a 10^{-4} M solution of the compound in 2-MeTHF at 18 K. The solvent was purified prior to use by passing it over an aluminum oxide column followed by refluxing in an N_2 atmosphere over calcium hydride and distilling. Both time-resolved and steady-state emission spectra were obtained for solid samples of the compound. The time-resolved emission spectra were taken at 18 K. The sample temperature was varied from 19 up to 79 K for the steady-state measurements.

Time-resolved emission spectra were obtained by using 480.0-nm pulsed excitation from a XeCl Excimer pumped dye laser (Coumarin 481 dye in *p*-dioxane). The signal was collected at approximately 45° from the excitation source. A 0.3-m monochromator and a gated diode array detector (OMA) interfaced to its own computer were used to collect, store, and display the spectra. A Model 1211 EG&G high-voltage pulse generator (low-limit pulse width of approximately 140 ns) triggered by the laser was used to gate the detector. The time-resolved emission spectra are not corrected for the system response.

Steady-state emission spectra were taken by using an Ar ion laser excitation source. The signal was collected at approximately 45° from the excitation beam, passed through a Spex 1702 0.75-m single monochromator, and then detected with an RCA C31034 photomultiplier tube. The signal from the photomultiplier tube was fed into an EG&G Model 1105 photon counter and stored digitally on an Apple II computer. Spectra were later transferred to a VAX 780 computer for analysis and display. All steady-state emission spectra are corrected for the system response. Correction factors were calculated by using Planck's formula for blackbody radiation in units of photons per unit volume per unit time and the measured output of a standard General Electric NBS 100-W, 120-V tungsten-filament lamp (T_c = 2859 K).

Raman Spectra. Room-temperature Raman spectra were obtained from a solid sample of *trans*-$W(N_2)_2(dppe)_2$ by using the 632.8-nm line of a helium–neon laser. The signal was collected at approximately 90° from the excitation beam. The data were collected, stored, and displayed by using an Instruments SA triple monochromator and a diode array detector (OMA) interfaced to its own computer. Additionally, the spectrum was obtained by using a Spex 1401 0.85-m double monochromator and an RCA C31034A02 photomultiplier tube interfaced to an EG&G Model 1105 photon counter. In this case, the data were stored and displayed by using an Apple II computer.

Lifetime Data. The emission lifetime of a solid sample of *trans*-$W(N_2)_2(dppe)_2$ was determined at 13 K by using 406.0-nm pulsed excitation (10 ns pulse width) from a XeCl Excimer pumped dye laser (DPS in *p*-dioxane). The signal was passed through a Spex 1702 single

---

(1) Caruana, A.; Kisch, H. *Angew. Chem., Int. Ed. Engl.* **1979**, *18*, 328.
(2) Brummer, J. G.; Crosby, G. A. *J. Phys. Chem.* **1984**, *88*, 6089.
(3) Brummer, J. G.; Crosby, G. A. *Inorg. Chem.* **1985**, *24*, 552.
(4) Caruana, A.; Hermann, H.; Kisch, H. *J. Organomet. Chem.* **1980**, *187*, 349.
(5) Chatt, J.; Head, R. A.; Leigh, G. J.; Pickett, C. J. *J. Chem. Soc., Dalton Trans* **1978**, 1638.
(6) Thomas, R. J. W.; Laurence, G. S.; Diamantis, A. A. *Inorg. Chim. Acta* **1978**, *30*, L353.
(7) Diamantis, A. A.; Chatt, J.; Leigh, G. J.; Heath, G. A. *J. Organomet. Chem.* **1975**, *84*, C11.
(8) Chatt, J.; Diamantis, A. A.; Heath, G. A.; Hopper, N. E.; Leigh, G. J. *J. Chem. Soc., Dalton Trans.* **1977**, 688.
(9) Tutt, L.; Zink, J. I.; Heller, E. J. *Inorg. Chem.* **1987**, *26*, 2158.
(10) Tutt, L.; Zink, J. I. *J. Am. Chem. Soc.* **1986**, *108*, 5830.
(11) Tutt, L.; Tannor, D.; Schindler, J.; Heller, E. J.; Zink, J. I. *J. Phys. Chem.* **1983**, *87*, 3017.
(12) Zink, J. I.; Tutt, L.; Yang, Y. Y. *ACS Symp. Ser.* **1986**, *No. 307*, 39.
(13) Preston, D. M.; Gunter, W.; Lechner, A.; Gliemann, G.; Zink, J. I. *J. Am. Chem. Soc.* **1988**, *110*, 5628.
(14) Preston, D. M.; Shin, K. S.; Hollingsworth, G.; Zink, J. I. *J. Mol. Struct.* **1988**, *173*, 185.
(15) Yang, Y. Y.; Zink, J. I. *Inorg. Chem.* **1985**, *24*, 4012.
(16) Chatt, J.; Heath, G. A.; Richards, R. L. *J. Chem. Soc., Dalton Trans.* **1974**, 2074.

0020-1669/89/1328-3519$01.50/0

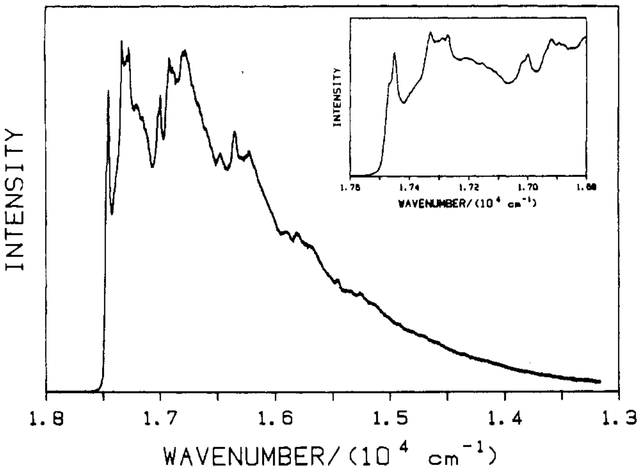

Figure 1. Luminescence spectrum of a solid sample of *trans*-$W(N_2)_2(dppe)_2$ at 19 K. The excitation wavelength was 514.5 nm. The inset shows an expanded view in the region near the origin.

Table I. Positions of the Most Prominent Peaks in the Emission Spectrum of *trans*-$W(N_2)_2(dppe)_2$[a]

position/cm^{-1}	diff/cm^{-1}	assgn[b]
17449	0	E_{00}
17384 (sh)[c]	65	ν_1
17326	123	ν_4
17268	181	ν_5
17206	243	$2\nu_4$
17152	297	$\nu_4 + \nu_5$
16994	455	ν_7
16920	529	ν_8
16876	573	$\nu_7 + \nu_4$
16801	648	$\nu_8 + \nu_4$
16473	976	$\nu_7 + \nu_8$
16348	1101	ν_{11}
16225	1224	$\nu_{11} + \nu_4$
15903	1546	$\nu_{11} + \nu_7$
15819	1630	$\nu_{11} + \nu_8$
15466	1983	ν_{13} and $\nu_{11} + 2\nu_7$
15258	2191	$2\nu_{11}$
17467 (sh)	0	E'_{00}
17289	178	ν_5
17013 (sh)	454	ν_7
16936 (sh)	531	ν_8
16891	576	$\nu_7 + \nu_4$
16775	692	$\nu_8 + \nu_5$ and $\nu_7 + 2\nu_4$

[a] See Figure 1. [b] See Table II. [c] sh = shoulder.

monochromator, detected by an RCA C31034 photomultiplier tube, and then collected and stored with a Tektronix RTD 710 transient digitizer interfaced to an IBM XT computer. The data were later transferred to a VAX 780 computer for analysis and display.

Mull Absorption Spectra. UV/vis halocarbon grease mull absorption spectra of *trans*-$W(N_2)_2(dppe)_2$ at both room temperature and 77 K were recorded with a Cary 219 spectrophotometer.

Results

(1) Emission Spectra. The steady-state emission spectrum of a solid sample of *trans*-$W(N_2)_2(dppe)_2$ taken at 19 K with 514.5-nm excitation is shown in Figure 1. The spectrum peaks at 17326 cm^{-1} and shows sharp-line vibronic structure with line widths as narrow as 15 cm^{-1}. The highest energy distinctly observed peak rises rapidly out of the base line at 17449 cm^{-1}. The inset shows an expanded view in the region of the origin. A doubling in the emission spectrum can be clearly observed in the expanded figure. A second, less intense feature is found at 17467 cm^{-1} as a high-energy shoulder on the first peak. Table I lists the positions of the most prominent peaks in the spectrum and their spacings in wavenumbers from either 17449 or 17467 cm^{-1}. The ratio of the intensities of these two features remains constant from 14 up to 27 K. At temperatures higher than 27 K the fine structure becomes less distinct, making ratio comparisons difficult. Emission spectra taken with 488.0- and 457.9-nm excitation showed all the features observed in the spectrum excited at 514.5 nm. However, the fine structure was slightly less resolved with the lower wavelength excitation.

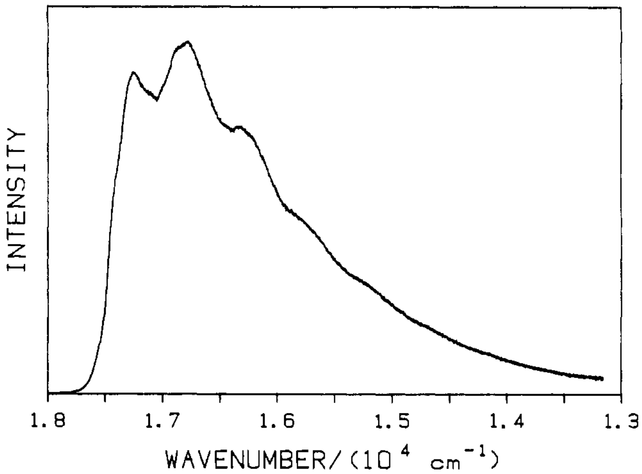

Figure 2. Luminescence spectrum of solid *trans*-$W(N_2)_2(dppe)_2$ at 79 K. The excitation wavelength was 514.5 nm.

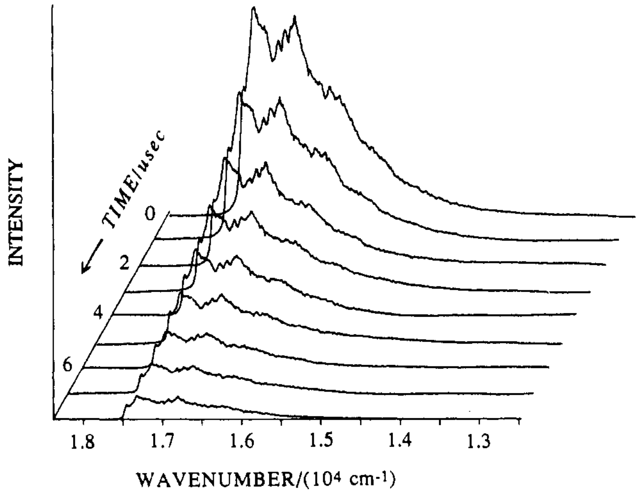

Figure 3. Time-dependent luminescence spectra of solid *trans*-$W(N_2)_2(dppe)_2$ at 18 K. A 200 ns sampling window was used. The delay time after the exciting laser pulse is shown.

The steady-state emission spectrum at 79 K obtained by using 514.5-nm excitation is shown in Figure 2. At 79 K the sharp-line vibronic structure has broadened, and the spectrum peaks at 16787 cm^{-1}. The relative intensities of the first two broad features in the spectrum reverse upon raising the temperature. The spacings between the broadened peaks are 446, 507, 517, and 528 ± 50 cm^{-1}.

The time-resolved spectrum of *trans*-$W(N_2)_2(dppe)_2$ in 2-MeTHF glass at 18 K exhibits a time dependence much like that observed by Brummer and Crosby.[3] A short-lived impurity emission, which disappears within 170 ns after excitation, is observed. After 170 ns, the spectral shape is invariant with time and the overall shape is the same as that observed for solid *trans*-$W(N_2)_2(dppe)_2$. The glass emission spectrum is blue-shifted by 500 cm^{-1} with respect to the solid spectrum. The vibronic structure is much broader compared to that in the solid emission spectrum. The sharp features with 15-cm^{-1} line widths are broadened to give one apparent progression. The vibronic spacings in the glass spectrum are the same as those observed in the 79 K solid spectrum.

Time-resolved emission spectra of the solid sample at 18 K were taken for comparison with those of the sample in the glass. As shown in Figure 3, the spectral shape obtained from the solid was found to be invariant with time. A 200-ns sampling window was used to measure the spectra shown. Since these spectra were taken with a 0.3-m monochromator, the experimental resolution is less than that obtained for the steady-state measurements.

Table II. Raman Vibrational Frequencies and Calculated Distortions for *trans*-$W(N_2)_2(dppe)_2$

freq/cm^{-1}	assgnt	distortion[a]
65	ν_1	0.92
80	ν_2	0.40
90	ν_3	0.35
125	ν_4	1.34
176 (179[b])	ν_5 (ν_{W-P})[b]	1.09
426 (414[b])	ν_6 (δ_{W-N_2})[b]	0.35
450 (442[b])	ν_7 (δ_{W-N_2})[b]	0.97
524 (524,[b] 525[c])	ν_8 (ν_{W-N})[b,c]	1.02
1000	ν_9 (phenyl ring)[d]	0.10
1027	ν_{10} (phenyl ring)[d]	0.20
1094	ν_{11} (phenyl ring)[d]	0.77
1584	ν_{12} (phenyl ring)[d]	0.35
2000 (1996[b])	ν_{13} (ν_{N-N})[b]	0.35

[a] Dimensionless distortion determined from the emission spectrum. [b] Reference 17. [c] Reference 3. [d] Reference 18.

(2) Raman Spectrum. The vibrational frequencies observed in the Raman spectrum of *trans*-$W(N_2)_2(dppe)_2$ with 632.8-nm excitation are listed in Table II. Included in this table are the frequencies previously reported by other workers.[3,17] Several vibrations not previously reported, including vibrations at 125 and 1094 cm^{-1} that are found in the emission spectrum, are observed.

(3) Emission Lifetime. The lifetime of the emission from solid *trans*-$W(N_2)_2(dppe)_2$ at 13 K was measured at 577.2 nm (17 325 cm^{-1}) and 591.0 nm (16 920 cm^{-1}). Plots of ln (intensity) versus time were linear over at least 2 decay lifetimes. The measured lifetimes are 4.5 ± 0.4 and 4.8 ± 0.4 μs at 577.7 and 591.0 nm, respectively, with an average of 4.6 ± 0.4 μs. This is less than the value of 19 μs previously reported by Caruana and Kisch[1] and the 21 μs lifetime reported by Brummer and Crosby.[3] However, both of these previous measurements were made from a 2-MeTHF glass at 77 K.

(4) Mull Absorption Spectra. The room-temperature and 77 K mull absorption spectra of *trans*-$W(N_2)_2(dppe)_2$ are essentially the same with a slight sharpening of the spectrum at 77 K compared to the room-temperature spectrum. The low-energy tail of the 77 K mull absorption spectrum overlaps with the onset of the solid-state emission at 79 K. The three lowest energy peaks observed in the 77 K mull absorption spectrum are at 18 868, 20 534, and 22 026 cm^{-1}. The previously reported absorption spectrum from a 2-MeTHF glass at 77 K is blue-shifted compared to the mull spectrum.[3]

Discussion

(1) Solid-State Emission. From the solid-state emission at 19 K the purely electronic transition, E_{00}, of *trans*-$W(N_2)_2(dppe)_2$ is assigned to the first distinctly observed highest energy peak at 17 449 cm^{-1} (see Figure 1). The high-energy shoulder at 17 467 cm^{-1} is assigned to a second, less intense origin, E'_{00}. The spacing between the two origins is 18 cm^{-1}. This doubling is observed throughout the spectrum. Table I lists the positions of the most prominent peaks, their differences in wavenumbers from E_{00} or E'_{00}, and the corresponding vibrational assignments for the peaks. Assignments are based upon the observed energy difference from the origin and on the calculated high-resolution spectrum (vide infra). The W–P and W–N vibrations are clearly observed at 181 and 529 cm^{-1} from E_{00}, respectively.[3,17] They are also observed at 178 and 531 cm^{-1} from E'_{00}. Additionally, peaks corresponding to Raman-determined vibrations at 65, 125, 450, and 1094 cm^{-1} are found. The vibration at 1094 cm^{-1} is assigned to an in-plane phenyl ring vibration that involves some movement of the phosphorus atom.[18] The vibration at 450 cm^{-1} is assigned to a W–N–N bending mode.[17] The vibrations at 65 and 125 cm^{-1} have not been assigned.

The cause of the doubling in the emission was investigated by measuring the spectrum's temperature dependence. There are two possible explanations for the doubling. Either there are two different sites within the crystal that emit at slightly different energies or emission is being observed from two different thermally equilibrated excited states within the molecule. On the basis of a thermally equilibrated Boltzmann distribution at 19 K, the population ratio of an upper state to a lower state with a separation of 18 cm^{-1} is 0.26. At 27 K the ratio is 0.38. The ratio of the intensities for the two origins, E_{00} and E'_{00}, is invariant with temperature from 19 to 27 K. From this temperature invariance, we conclude that the double origin arises from different sites within the crystal that emit at slightly different energies.

(2) Time-Dependent Theory of Emission Spectroscopy. *trans*-$W(N_2)_2(dppe)_2$ represents a case where a multidimensional analysis of the emission spectrum is necessary. Thirteen different vibrational modes contribute to the emission spectrum. The time-dependent theory of molecular spectroscopy developed by Heller can easily treat multidimensional cases.[10] Additionally, the progression observed in the glass and in the 79 K solid-state spectra can be understood from the viewpoint of the time-dependent theory as a MIME.[10-15] Because the mathematical development of the time-dependent theory has been treated in detail elsewhere, only a brief discussion of the theory as it applies to emission spectroscopy will be given here.[19,20]

A molecular emission spectrum is the Fourier transform of the time-dependent overlap of an initial wave function with a time-dependent wave function.[19] The initial wavepacket, ϕ_k, is an eigenfunction of the lowest vibrational level of the lowest energy excited-state potential surface. The emission process corresponds to the wavepacket making a vertical transition from this state down to the ground-electronic-state surface whose minimum is displaced from the upper surface by an amount Δ_k along the kth normal coordinate. The wavepacket is not a stationary state of the ground-state potential energy surface, and once on this surface, it begins to propagate according to the time-dependent Schrödinger equation. The overlap, $\langle\phi_k|\phi_k(t)\rangle$, of the time-dependent wave function, $\phi_k(t)$, with the initial wave function, ϕ_k, is the quantity of interest. At $t = 0$ the overlap is 1. As the wavepacket moves away from its initial position, the overlap decreases and eventually goes to zero. At a later time, t, corresponding to the period of oscillation for the kth normal mode, the wavepacket will return to its initial position, giving rise to a recurrence in the overlap. Under the assumptions of harmonic potentials, no Duschinsky effect, the same ground- and excited-state force constants, and the Condon approximation, the following simple expression for the overlap function is obtained:[11,19]

$$|\langle\phi_k|\phi_k(t)\rangle| = \exp[-(1/2)\Delta_k^2(1 - e^{-i\omega_k t}) - i\omega_k t/2] \qquad (1)$$

where Δ_k is the dimensionless equilibrium distortion of the first excited state in the kth normal mode and ω_k is its vibrational frequency. Because the potential surfaces are displaced along more than one normal mode, the total overlap is the product of the overlap functions for each normal mode:[11,19]

$$|\langle\phi|\phi(t)\rangle| = \prod_k \langle\phi_k|\phi_k(t)\rangle \exp(-iE_{00}t/\hbar - \Gamma^2 t^2) \qquad (2)$$

where E_{00}, the electronic shift between the minima of the excited- and ground-state potential energy surfaces, and Γ, a Gaussian damping factor, are now included. The emission spectrum is the Fourier transform of the time domain function:[11,19]

$$I(\omega) = C\omega^3 \int_{-\infty}^{\infty} e^{i\omega t}\{\langle\phi|\phi(t)\rangle\}\,dt \qquad (3)$$

where C is a constant and $I(\omega)$ is the intensity in photons per unit volume per unit time at frequency ω.

The damping factor Γ plays an important role in the spectrum. Damping of the molecular wave function occurs because of relaxation of the wavepacket into other modes or into the thermal bath. This results in a decrease in the magnitudes of subsequent recurrences in the overlap compared to the initial overlap at $t = 0$. When Γ is greater than zero, the overlap at t is less than the

---

(17) Colquhoun, H. M.; Head, R. A. *Inorg. Chim. Acta* **1980**, *45*, L123.

(18) Whiffen, D. H. *J. Chem. Soc.* **1956**, 1350.

(19) Tannor, D. J.; Heller, E. J. *J. Chem. Phys.* **1982**, *77*, 202.

(20) Heller, E. J. *Acc. Chem. Res.* **1981**, *14*, 368.

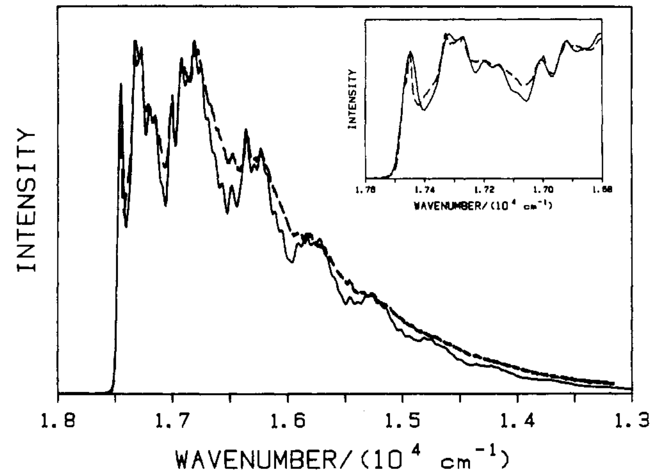

Figure 4. Experimental (--) and calculated (—) emission spectra of *trans*-$W(N_2)_2(dppe)_2$ at 19 K. The calculated spectrum was obtained by using the distortions given in Table II; E_{00} = 17 449 cm^{-1}, and Γ = 17.5 cm^{-1}. The inset compares the expanded spectra in the region near the origin.

overlap at $t = 0$. In the frequency domain this results in a less resolved spectrum. At high Γ no recurrences in the overlap are observed. The result in the frequency domain is a completely filled in spectrum where all that is observed is the broad envelope.

(3) Calculated Emission Spectrum and Excited-State Distortions. The high-resolution emission spectrum of *trans*-$W(N_2)_2(dppe)_2$ was calculated by using eq 1–3. The frequencies of the vibrational modes and E_{00} were obtained from the Raman and the experimental emission spectra, respectively. The damping factor, Γ, and the distortions, Δ_k, were varied to give the best fit to the line widths and intensity distributions observed in the experimental spectrum.

The experimental and calculated spectra are compared in Figure 4. The inset compares the expanded spectra in the region near the origin. In the calculation an E_{00} of 17 449 cm^{-1} was used. The calculation therefore only produces the spectrum on the basis of this main origin. A damping factor of Γ = 17.5 cm^{-1} was found to give the best overall fit to the experimental line widths. The vibrational modes and distortions (dimensionless) used in the calculation are summarized in Table II. The molecule undergoes small distortions along 13 normal coordinates in its first excited state. The small distortions are consistent with the overall shape of the spectrum in which the vibrational progression intensities peak within the first quanta of the progression. Six vibrational modes at 65, 125, 176, 450, 524, and 1094 cm^{-1} are the major contributors to the emission spectrum. The distortion along ν_{11} (1094 cm^{-1}), the phenyl ring normal mode that involves some movement of the phosphorus atom attached to the ring,[18] is of comparable magnitude to the metal–ligand distortions. The calculation gives a good fit to the experimental spectrum; not only are the main features in the spectrum reproduced, but also several weaker features corresponding to various overtone and combination bands observed in the lower energy region of the spectrum are reproduced as well.

The major source of uncertainty in the calculated molecular distortions is caused by the doubling in the experimental spectrum. The experimental spectrum is less highly resolved than the calculated spectrum because the double origin causes some filling in of the experimental spectrum that is not reproduced in the calculation. The distortions that are calculated most accurately are those for the modes with relatively large displacements. These are the modes that are the major contributors to the peaks observed in the emission spectrum (i.e. ν_1, ν_4, ν_5, ν_7, ν_8, and ν_{11}). The calculated distortions are unique to within $\pm 0.05\Delta_k$ for these modes. The remaining modes, with relatively small displacements, primarily serve to fill in the spectrum, and the uncertainty in determining their distortions is larger.

Converting the dimensionless distortions into angstrom units requires a full normal-coordinate analysis of the molecule. Since such an analysis has not been completed, a few simple assumptions about the geometry of the molecule and the masses involved will be used to give an estimate of the distortions. Assuming a D_{4h} local symmetry about the central tungsten atom, an isolated N–N oscillator for the N–N coordinate, and molar atomic masses of 14.0, 28.0, and 199.2 g (half the mass of the dppe ligand) for the N–N, W–N, and W–P normal coordinates, respectively, the calculated distortions are 0.01, 0.05, and 0.03 Å along the N–N, W–N, and W–P coordinates.[21] For the W–N and W–P normal coordinates, the relationships between the change in bond length, δ, and the normal-coordinate distortion, Δ, are

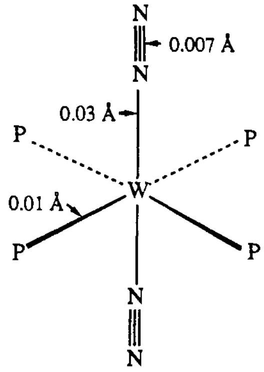

Figure 5. Changes in bond lengths of *trans*-$W(N_2)_2(dppe)_2$ in its first excited state. The local D_{4h} geometry of the tungsten atom is emphasized by omitting the carbon and phenyl groups attached to the phosphorus atoms. Each W–N, W–P, and N–N bond is distorted by 0.03, 0.01, and 0.007 Å, respectively.

$$\Delta(\text{W–N}) = \left(\sqrt{2}/2\right)[\delta(\text{W–N})_1 + \delta(\text{W–N})_2] \qquad (4)$$

$$\Delta(\text{W–P}) = (1/2)[\delta(\text{W–P})_1 + \delta(\text{W–P})_2 + \delta(\text{W–P})_3 + \delta(\text{W–P})_4] \qquad (5)$$

The W–N and W–P bond length changes determined by using eq 4 and 5 are 0.03 and 0.01 Å, respectively. A similar conversion gives a change of 0.007 Å for the N–N bond. The individual bond length changes are summarized in Figure 5.

(4) The Missing-Mode Effect. The spectra of *trans*-$W(N_2)_2(dppe)_2$ provide an excellent example of the missing-mode effect.[10-15] In 2-MeTHF glass at temperatures between 8 and 80 K the sharp-line vibronic structure is unresolved and the spectrum appears to contain a single progression with a spacing of approximately 500 cm^{-1}.[3] In the solid sample at 79 K this single progression is also observed. Lowering the temperature resolves new features that cannot be observed in the glass spectrum (see Figures 1 and 2). These features are used to quantify the MIME frequency.

The MIME is best understood from the viewpoint of the time-dependent theory.[19,20] In the time domain, two or more vibrational modes can combine to give a partial recurrence in $\langle\phi|\phi(t)\rangle$ at $t = t_m$, which is not possible from any one mode alone. This partial recurrence at t_m results in the MIME progression with a spacing of ω_m in the frequency domain. A requirement for the appearance of the MIME is that the spectrum must not be fully resolved. In other words, the damping factor, Γ, must be large. When Γ is small, there will be many recurrences of the overlap in the time domain and the emission spectrum will exhibit sharp, well-defined vibronic structure. Progressions in the normal modes and combination bands will be observed. The time-dependent overlap for the calculation of the low-temperature, highly resolved

---

(21) The conversion from dimensionless units into angstrom units uses the formula

$$D = (Nh/4\pi^2 c\omega m)^{1/2} \times \Delta 10^8 \text{ Å/cm}$$

where D is the distortion in the normal coordinate in Å, Δ is the distortion in the normal coordinate in dimensionless units, N is Avogadro's number, h is Planck's constant in g cm^2 s^{-1}, c is the speed of light in cm s^{-1}, ω is the frequency of the mode in cm^{-1}, and m is the molar atomic mass for the mode in g.

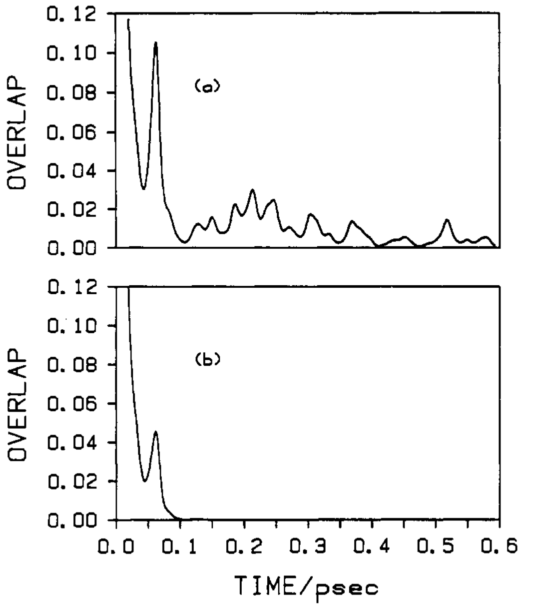

Figure 6. Time dependence of the overlap for the calculated spectra shown in Figures 4 and 7: (a) $\Gamma = 17.5$ cm^{-1}; (b) $\Gamma = 80$ cm^{-1}.

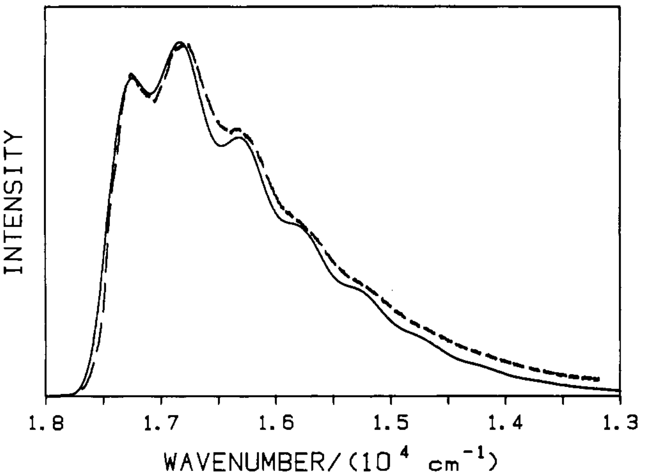

Figure 7. Experimental (- -) and calculated (—) emission spectra of *trans*-W$(N_2)_2$(dppe)$_2$ at 79 K. The calculated spectrum was obtained by using the distortions given in Table II; $E_{00} = 17\,449$ cm^{-1}, and $\Gamma = 80$ cm^{-1}.

solid-state spectrum (see Figure 4) where $\Gamma = 17.5$ cm^{-1} is shown in Figure 6a. In this case, the overlap function contains many recurrences. If Γ is increased (to 80 cm^{-1}, for example), the recurrences at long times are damped out and the spectrum is filled in. The MIME can occur under these conditions. The time-dependent overlap using the same distortions as those used for Figure 6a and a Γ of 80 cm^{-1} is shown in Figure 6b. In this case, the long time recurrences are damped out, leaving only one prominent recurrence at $t = t_m = 0.06$ ps.

The emission spectrum of solid *trans*-W$(N_2)_2$(dppe)$_2$ at 79 K is completely calculated from eq 1–3 by using exactly the same distortions as those used for the 19 K spectrum. The only change in the calculation was an increase in Γ to 80 cm^{-1}. Figure 7 compares the calculated and experimental spectra for this case. The calculated spectrum is the Fourier transform of the overlap shown in Figure 6b. Again, the calculation gives a good fit to the experimental spectrum. The relative intensities and positions of the peaks are reproduced. The decrease in intensity of the first main vibrational peak relative to the second in going from 19 to 79 K is a result of broadening the narrow peaks at 17 326, 17 289, and 17 268 cm^{-1}, which contribute to the first main vibrational peak.

The high-resolution spectrum allows the distortions for *trans*-W$(N_2)_2$(dppe)$_2$ in its first excited electronic state to be accurately determined. In cases where a high-resolution spectrum cannot be obtained, the distortions can be calculated from the preresonance Raman spectrum.[10–12,15] For both cases, the calculated normal-coordinate distortions can be used to quantitatively describe the MIME.

(5) Comparison with Previous Experiments. The lowest energy emitting state of *trans*-W$(N_2)_2$(dppe)$_2$ has been previously assigned to a spin-forbidden transition from a metal to a dppe charge-transfer excited state.[1–3] The results discussed above are consistent with this assignment. First, the 500-cm^{-1} blue shift of the emission spectrum in 2-MeTHF compared to that from the solid is characteristic of solvent dependencies observed in charge-transfer transitions.[22,23] The absorption spectrum in 2-MeTHF at 77 K is blue-shifted with respect to the mull absorption spectrum. Moreover, the origin of the emission from the solid sample at 79 K overlaps with the origin of the 77 K mull absorption spectrum. Therefore, trap emission is not a major cause of the 500-cm^{-1} shift, and we attribute this shift to medium effects on the charge-transfer state. Second, the small calculated distortions are consistent with this assignment. Much larger distortions would be expected along the metal–ligand normal modes (e.g. 0.1–0.2 Å)[10] if the emitting state were ligand field in character. Further support for the charge-transfer assignment comes from the comparable magnitude of the distortion in the phenyl ring mode ν_{11} with the distortions in the metal–ligand modes. Last, the 4.6-μs emission lifetime of *trans*-W$(N_2)_2$(dppe)$_2$ in the solid state at 13 K, although shorter than the previously reported lifetime in 2-MeTHF at 77 K,[1,3] is consistent with the spin-forbidden assignment. The different lifetimes are probably caused by medium effects.

Time-resolved emission spectra of *trans*-W$(N_2)_2$(dppe)$_2$ were obtained to determine if impurity emissions were present in the sample. Brummer and Crosby found a short-lived impurity emission along with the longer lived *trans*-W$(N_2)_2$(dppe)$_2$ emission in the 2-MeTHF glass spectrum.[3] Repeating their experiment by using a gated OMA yielded similar results. In contrast, the emission spectrum of the solid is invariant with time. *trans*-W$(N_2)_2$(dppe)$_2$ is highly photoreactive when in solution.[4–8] The impurity emission observed in 2-MeTHF glass is possibly the result of photogenerated reaction product(s) that are produced when the sample is solvated. The nature of this impurity was not further investigated.

Acknowledgment. We gratefully acknowledge the support of the National Science Foundation (Grant CHE 88-06775) and thank Professor H. Kisch for the gift of the title compound.

---

(22) Wrighton, M.; Morse, D. L. *J. Am. Chem. Soc.* **1974**, *96*, 998.
(23) Lees, A. J. *Chem. Rev.* **1987**, *87*, 711.